The Astrophysical Journal, 833:9 (6pp), 2016 December 10 doi:10.3847/0004-637X/833/1/9

MILLIMETER/SUBMILLIMETER SPECTROSCOPY OF TiO ($X^3\Delta_r$): THE RARE TITANIUM ISOTOPOLOGUES

A. P. Lincowski, D. T. Halfen, and L. M. Ziurys
Department of Chemistry and Biochemistry, Department of Astronomy, and Steward Observatory, University of Arizona, 1305 E. 4th Street, Tucson, AZ 85719, USA; lziurys@email.arizona.edu
Received 2016 August 4; revised 2016 September 21; accepted 2016 September 27; published 2016 December 1

ABSTRACT

Pure rotational spectra of the rare isotopologues of titanium oxide, ^{46}TiO, ^{47}TiO, ^{49}TiO, and ^{50}TiO, have been recorded using a combination of Fourier transform millimeter-wave (FTmmW) and millimeter/submillimeter direct absorption techniques in the frequency range 62–538 GHz. This study is the first complete spectroscopic characterization of these species in their $X^3\Delta_r$ ground electronic states. The isotopologues were created by the reaction of N_2O or O_2 and titanium vapor, produced either by laser ablation or in a Broida-type oven, and observed in the natural Ti isotopic abundances. Between 10 and 11 rotational transitions $J+1 \leftarrow J$ were measured for each species, typically in all 3 spin–orbit ladders $\Omega = 1$, 2, and 3. For ^{47}TiO and ^{49}TiO, hyperfine structure was resolved, originating from the titanium-47 and titanium-49 nuclear spins of $I = 5/2$ and 7/2, respectively. For the $\Omega = 1$ and 3 components, the hyperfine structure was found to follow a classic Landé pattern, while that for $\Omega = 2$ appeared to be perturbed, likely a result of mixing with the nearby isoconfigurational $a^1\Delta$ state. The spectra were analyzed with a case (a) Hamiltonian, and rotational, spin–orbit, and spin–spin parameters were determined for each species, as well as magnetic hyperfine and electric quadrupole constants for the two molecules with nuclear spins. The most abundant species, ^{48}TiO, has been detected in circumstellar envelopes. These measurements will enable other titanium isotopologues to be studied at millimeter wavelengths, providing Ti isotope ratios that can test models of nucleosynthesis.

Key words: astrochemistry – ISM: molecules – line: identification – methods: laboratory: molecular – molecular data

Supporting material: machine-readable table

1. INTRODUCTION

Titanium has been described as the richest element in which to study theories of nucleosynthesis (e.g., Clayton 2003). In part because it is refractory, the element has also played a significant role in planetary science and meteorite analyses (e.g., Greber et al. 2016). The scientific importance of titanium is linked to its five stable isotopes: ^{48}Ti, ^{46}Ti, ^{47}Ti, ^{49}Ti, and ^{50}Ti, as well as to a radioactive isotope, ^{44}Ti, which can be studied by X-ray emission (e.g., Miceli et al. 2015). The five isotopes, which have abundances of 73.7%, 8.3%, 7.4%, 5.4%, and 5.2%, respectively, are produced by a variety of nucleosynthetic processes, including explosive and hydrostatic oxygen and silicon burning in massive stars, slow neutron capture (s-process) in the AGB phase, and in SNe Type Ia (Clayton 2003). For example, models predict significant overproduction of the neutron-rich species ^{49}Ti and ^{50}Ti in the cores of massive stars that will become supernovae (Prantzos et al. 1987). Titanium isotope ratios have thus been used to identify the origin of pre-solar grains (e.g., Nittler & Hoppe 2005) or to study s-process enrichments in stellar photospheres (Wyckoff & Wehinger 1972).

One approach by which titanium isotopes can be studied in interstellar and circumstellar gas is by Ti-bearing molecules. One particularly good candidate is TiO. This species has been observed in the photospheres of red giant stars for decades, particularly via its $A^3\Phi$–$X^3\Delta$ electronic transition near 7000 Å (e.g., Wyckoff & Wehinger 1972; Wade & Horne 1988). TiO electronic bands are sufficiently prominent in stellar photospheres of O-rich stars for them to be used for classification purposes (Morgan & Keenan 1973). In fact, a titanium isotopic analysis using TiO spectra has been conducted toward the Mira variable o Ceti (Wyckoff & Wehinger 1972). Upper limits to the ^{46}Ti/^{48}Ti, ^{47}Ti/^{48}Ti, ^{49}Ti/^{48}Ti, and ^{50}Ti/^{48}Ti ratios were obtained, which suggested an s-process enhancement of ^{50}Ti. More recently, TiO has been observed at millimeter wavelengths toward the circumstellar envelope of supergiant star VY Canis Majoris, or VY CMa (e.g., Kaminski et al. 2013). This discovery helps link photospheric and circumstellar molecules. TiO, along with TiO_2, have now been observed toward VY CMa with the Atacama Large Millimeter Array (ALMA), which has elucidated their spatial distributions around this massive star (e.g., De Beck et al. 2015).

In part because of its astrophysical importance, TiO has been a subject of laboratory gas-phase spectroscopy for decades, with a particular focus on electronic transitions (see Merer 1989 for a review). Further studies occurred in the 1990s. Amiot et al. (1995), for example, conducted laser-induced fluorescence (LIF) measurements of the $B\,^3\Pi$–$X^3\Delta$ (1, 0) band, and established the most accurate values for spin–orbit and spin–spin constants A and λ for the ground state to date. The $C^3\Delta - a^1\Delta$ and $C^3\Delta - X^3\Delta$ transitions were investigated by Kaledin et al. (1995), while the $a^1\Delta$ and $b^1\Pi$ states were studied in the infrared by Ram et al. (1996). Fletcher et al. (1993) also used LIF to record the B–X transition of ^{47}TiO, and established estimates of the a, b, and eQq_0 hyperfine parameters of this species. Shortly thereafter, Barnes et al. (1996) measured the A–X band with double-resonance LIF, and partially resolved hyperfine splittings in ^{47}TiO and ^{49}TiO. In addition, the pure rotational spectrum of ^{48}TiO has been measured using pump/probe microwave optical double-resonance techniques by Namiki et al. (1998), who established a precise set of rotational constants for the main isotopologue.

More recently, the $E\,^3\Pi$–$X^3\Delta$ transition has been studied using frequency-modulated laser absorption methods in the near-infrared (Kobayashi et al. 2002); in this work, spectroscopic constants for the excited E state were determined. The $B^3\Pi$ state has been extensively characterized by Amiot et al. (2002), as well.

Because of the astrophysical interest in TiO, and the possibility of further studies with ALMA, we have conducted millimeter/submillimeter direct absorption and Fourier transform millimeter-wave (FTmmW) measurements of the other four isotopologues of titanium oxide: ^{46}TiO, ^{47}TiO, ^{49}TiO, and ^{50}TiO, all in their $^3\Delta_r$ ground electronic states. These are the first pure rotational studies of these species. Extensive titanium hyperfine structure was observed in two isotopologues, arising from the ^{47}Ti and ^{49}Ti nuclear spins of 5/2 and 7/2, respectively. Rotational and fine-structure constants have been determined for all four species, as well as hyperfine parameters for ^{47}TiO and ^{49}TiO. In this paper we present our measurements and spectroscopic analyses, and discuss the implications of our results.

2. EXPERIMENTAL

The measurements of the isotopologues of TiO were initially conducted with the FTMmmW spectrometer of the Ziurys group. This system is a Balle-Flygare-type design consisting of two spherical mirrors forming a Fabry–Perot cavity, housed in a vacuum chamber evacuated to 10^{-8} Torr by a cryopump (see Sun et al. 2009). The spectrometer operates from 4 to 90 GHz, using two different sets of mirrors and electronics; for the TiO study, only the higher frequency capability was used (40–90 GHz). In this case, waveguide is imbedded in each mirror for injection and subsequent detection of millimeter-wave radiation. The frequency source is a signal generator (Agilent), coupled with an active doubler (Norden Millimeter). The cavity supports radiation at a given frequency with an instantaneous bandwidth of ~1 MHz. Molecules are injected into the cavity in a supersonic expansion created by a pulsed nozzle oriented 40° with respect to the optical axis. If there is a transition in the given frequency range, the molecules absorb the radiation and then spontaneously emit. Detection of the short-lived (~40–50 μs) molecular emission (free induction decay, or FID) is accomplished in the time-domain using a low-noise amplifier (NRAO). An FFT of the FID signal generates a spectrum. Frequency ranges are scanned by changing the synthesizer frequency while optimizing the cavity response. All spectra exhibit a Doppler doublet structure owing to the arrangement of the beam relative to the electric field created in the cavity. The transition frequency is the average of the Doppler doublets.

TiO, a free radical, was created in the FTmmW instrument in a supersonic expansion coupled with a laser ablation source. A mixture of approximately 0.1% N_2O in 200 psi of argon was pulsed from the expansion nozzle (backing pressure of 40 psi) and flowed across a rotating/translating titanium rod, from which metal vapor was ablated by a Nd:YAG laser (532 nm). A DC discharge was not necessary to create TiO, unlike many other radical species (e.g., Min et al. 2014).

Higher frequency measurements of TiO were carried out with the high temperature, millimeter/submillimeter spectrometer of the Ziurys group. This direct-absorption instrument consists of a frequency source, a reaction cell containing a Broida-type oven, and a detector. Millimeter-wave radiation was produced using combinations of Gunn oscillators and Schottky diode multipliers to provide a near-continuous frequency coverage of approximately 65–850 GHz. The radiation output is launched quasi-optically from a scalar feed horn. It is directed by a series of lenses/mirrors, a polarizing grid, a pathlength modulator, and a rooftop reflector through the water-cooled reaction chamber, which is a double-pass system, and into the detector, a He-cooled InSb bolometer. Phase-sensitive detection at $2f$ is employed by FM modulation of the Gunn oscillator, resulting in second-derivative line shapes. For more details, see Ziurys et al. (1994).

Creation of TiO in the millimeter-wave system was accomplished by reacting either oxygen or nitrous oxide with titanium vapor, generated by the Broida oven. Approximately 1 mtorr of the reactant gas (N_2O or O_2—either worked well) was introduced above the top of the oven, while argon (25–30 mtorr) was inserted below the oven. The oven itself required special preparation to successfully vaporize titanium, which has a melting point near 1650°C. The oven electrodes were constructed from molybdenum, as opposed to steel, and the crucibles used, which are resistively heated in a tungsten basket (power ~750 W), were made of boron nitride, not the usual alumina. A high-purity (>99% pure) titanium rod was used, cut into small pieces. Several layers of insulation were packed around the crucible, the innermost layer created from zirconium felt and the outer layer from old alumina crucible fragments. Most importantly, zirconium felt was placed on the bottom of the basket to insulate the crucible from the heating element; otherwise, the bottom of the crucible would melt. No DC discharge was required to synthesize TiO.

Transition frequencies were obtained from averages of scans 5 MHz in width, with an equal number in increasing and decreasing frequency. One to ten scan averages were typically needed to obtain a reasonable signal-to-noise ratio. Each line was fit with a Gaussian profile to determine the central line frequency. For both spectrometers, all four isotopologues of TiO were observed in their natural abundance.

3. RESULTS

Because there were no estimates of spectroscopic parameters for the four less abundant isotopologues of titanium oxide, transition frequencies were predicted from rotational constants scaled from those of ^{48}TiO (Namiki et al. 1998). The initial search for the ^{46}Ti, ^{47}Ti, ^{49}Ti, and ^{50}Ti isotopologues of TiO was conducted with the FTmmW system. The ground state of TiO is $^3\Delta_r$; thus, there are three spin–orbit ladders in this molecule, labeled $\Omega = 1$, 2, and 3, each with its own rotational manifold with $J \geqslant \Omega$. The three spin ladders have a total energy separation of $4A$, or ~200 cm^{-1}, where A is the spin–orbit constant equal to ~50 cm^{-1}. Because of the supersonic cooling in the jet expansion of the FTmmW instrument, it is expected that only the lowest energy spin–orbit ladder, $\Omega = 1$, will be observed. As a consequence, the lowest rotational line of this substate, $J = 2 \rightarrow 1$ near 63 GHz, was searched for in the four rare isotopologues. The $J = 2 \rightarrow 1$ transition was readily found for both ^{46}TiO and ^{50}TiO, as each consisted of a single line and was within 10 MHz of the predictions. However, ^{47}TiO and ^{49}TiO have nuclear spins, ^{47}Ti ($I = 5/2$) and ^{49}Ti ($I = 7/2$), as mentioned. Spectral features were identified for these species, but the assignment was problematic. It was clear that the measurement of other transitions was imperative, and the study was continued with

Table 1
Observed Rotational Transitions of TiO Isotopologues ($X\,^3\Delta_r$)

							$\Omega = 1$		$\Omega = 2$		$\Omega = 3$	
Species	J'	↔	J''	F'	↔	F''	ν_{obs}	$\nu_{obs}-\nu_{calc}$	ν_{obs}	$\nu_{obs}-\nu_{calc}$	ν_{obs}	$\nu_{obs}-\nu_{calc}$
^{46}TiO	2	→	1				63991.702	−0.009				
	7	←	6				223955.847	0.077	226569.275	−0.017	228832.530	0.027
	8	←	7				255943.626	−0.012	258926.976	0.012	261511.405	0.028
	9	←	8				287929.197	0.029	291280.896	0.005	294185.658	−0.008
^{47}TiO	7	←	6	9.5	←	8.5	222728.731	0.110	225338.470	0.074	227617.711	0.128
				8.5	←	7.5	222735.651	0.009	225329.738	0.092	227579.901	0.044
				7.5	←	6.5	222741.610	−0.017	225322.484	−0.032	227549.222	−0.013
				6.5	←	5.5	222746.842	−0.017	225317.266	0.155	227525.625	0.110
				5.5	←	4.5	222751.503	−0.050	225313.418	−0.080	227508.594	0.083
				4.5	←	3.5	222755.780	−0.081	225311.670	−0.042	227497.989	−0.060

Notes. Frequencies in MHz.
[a] Blended line, not included in the fit.
[b] Beyond the range of the frequency source; not measured.

(This table is available in its entirety in machine-readable form.)

the millimeter/submillimeter spectrometer in the 219–538 GHz range. In this case, all three spin components were expected to be observed, as high temperatures were required to vaporize titanium.

Because of the complexities due to the fine and hyperfine structure, searches over broad frequency regions were conducted in the range 220–540 GHz. In the course of the search, multiple rotational transitions, beginning with $J = 7 \leftarrow 6$, were identified for all three spin–orbit components $\Omega = 1$, 2, and 3 for ^{46}TiO and ^{50}TiO, where $I = 0$. Typically, lines were found within 50 MHz of the predicted frequencies. However, features arising from N_2O and other oxygen-bearing contaminants made line identification somewhat challenging. For ^{47}TiO and ^{49}TiO, transitions were located on the basis of the sextet and octet patterns generated by their respective nuclear spins. However, depending on the spin component, these patterns were often distorted, as we discuss below. Spectral lines from these two species were usually found within 200 MHz of the predictions. Once the higher frequency hyperfine patterns of ^{47}TiO and ^{49}TiO were identified and understood, additional hyperfine components were measured with the FTmmW spectrometer.

The rotational frequencies measured for the four rare isotopologues of TiO ($X^3\Delta_r$) are listed in Table 1. Ten to eleven rotational transitions $J + 1 \leftrightarrow J$ were measured for each species, spanning the frequency range 62–538 GHz. Typically, all three fine-structure components ($\Omega = 1, 2, 3$) were measured for each transition, except for the $J = 2 \rightarrow 1$ line. In addition, six hyperfine components $F + 1 \leftrightarrow F$ were usually recorded for ^{47}TiO for each Ω component, and eight such lines for ^{49}TiO. No evidence of Λ-doubling was observed in any spectra, although this splitting has been reported in the two lowest energy transitions of the $\Omega = 1$ component of the main isotopologue by Namiki et al. (1998); the lambda-doubling was extremely small (4–10 kHz) and would be expected to be even smaller in the other spin–orbit ladders (Brown and Carrington 2003). In total, 387 individual lines were measured and included in the final analysis.

Representative spectra of the TiO isotopic species in their respective $X^3\Delta_r$ states are shown in Figures 1–4. In Figure 1, the millimeter-wave direct absorption spectra of the $J = 14 \leftarrow 13$ transition of ^{46}TiO are displayed near 447–457 GHz. The three spin components $\Omega = 1$, 2, and 3 are presented in separate panels. Although separated by over 200 cm^{-1} in energy, the intensities of these features are similar because of the high temperature of the reaction mixture.

In Figure 2, the millimeter-wave direct absorption spectra of the $J = 14 \leftarrow 13$ transition of ^{49}TiO are displayed near 440–450 GHz. The octet of hyperfine features, labeled F, is clearly discernible in the $\Omega = 1$ and 3 components as classic Landé patterns (upper and lower panels), where the frequency spacing is proportional to the quantum number F (note the interloping feature that is due to N_2O). The ordering of the transitions $F + 1 \leftarrow F$ is reversed for the two patterns, however, and their spacing varies. For the $\Omega = 2$ sublevel, the octet is not as obvious as the lower F components are essentially collapsed together. At lower J, the octet is clearly present, as shown in Figure 3. Here the millimeter-wave spectrum of the $J = 9 \leftarrow 8$, $\Omega = 2$ transition of ^{49}TiO is displayed near 286 GHz. As the figure illustrates, the frequency spacing steadily declines with decreasing F quantum number. An identical situation was found for the sextet in ^{47}TiO; see Table 1.

Figure 4 shows the FTmmW spectrum of the $J = 2 \rightarrow 1$ transition of ^{47}TiO in the lowest energy spin–orbit component, $\Omega = 1$, near 63 GHz. Here the seven measured hyperfine transitions are all displayed, labeled by the quantum number F. The Doppler doublets are indicated with brackets, and there are six frequency breaks in the data to show all seven features.

4. ANALYSIS

The data for the four isotopologues were analyzed separately in individual fits using a Hund case (a) effective Hamiltonian for a $^3\Delta$ state. This Hamiltonian includes molecular frame rotation, spin–orbit coupling, and spin–spin interactions, as well as magnetic hyperfine and electric quadrupole terms for ^{47}TiO and ^{49}TiO:

$$\hat{H}_{eff} = \hat{H}_{rot} + \hat{H}_{so} + \hat{H}_{ss} + \hat{H}_{mhf} + \hat{H}_{eQq}. \quad (1)$$

Matrix elements include those that are off-diagonal in J and Ω, as described in detail in Azuma et al. (1989). In the analysis, the data were weighted by the corresponding experimental precision (50 kHz versus 2 kHz). For all species, the values of the spin–orbit constant A and the spin–spin constant λ were

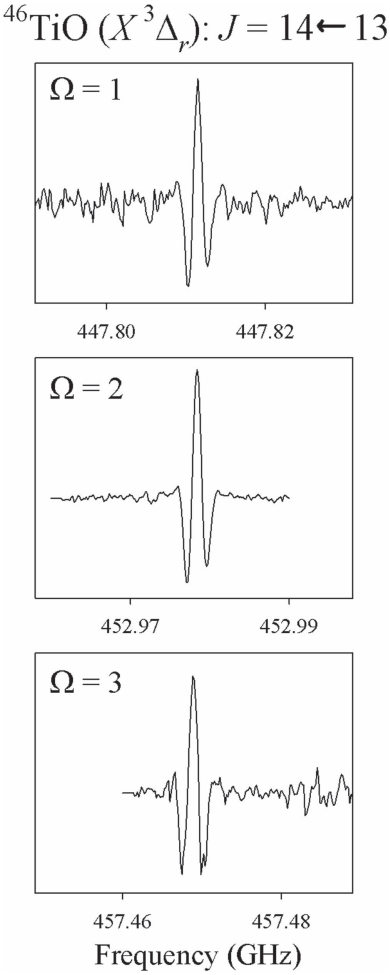

Figure 1. Millimeter/submillimeter direct absorption spectrum of the $J = 14 \leftarrow 13$ rotational transition of ^{46}TiO ($X^3\Delta_r$) near 447–457 GHz, displaying all three spin–orbit ladders, $\Omega = 1$, 2, and 3. These components span ~200 cm^{-1} in energy, but have similar intensities because of the extreme conditions needed to vaporize titanium. The spectra were recorded as single scans with a duration of 70 s and widths of 110, 30, and 30 MHz, respectively.

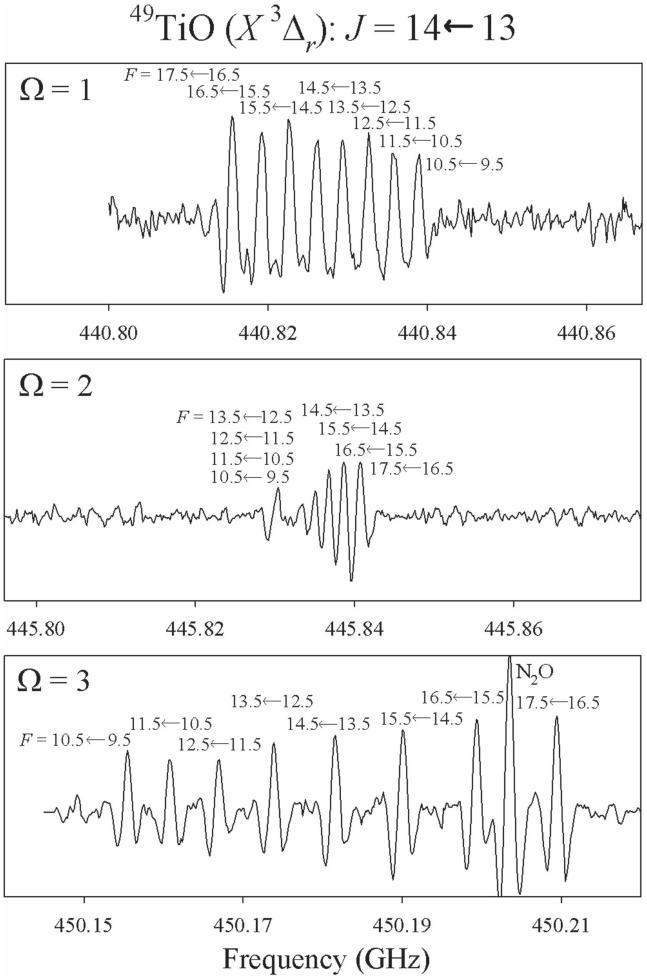

Figure 2. Millimeter/submillimeter direct absorption spectrum of the $J = 14 \leftarrow 13$ rotational transition of ^{49}TiO ($X^3\Delta_r$) near 440–450 GHz, displaying all three Ω ladders. Each spin–orbit component exhibits an octet structure that is due to the nuclear spin of ^{49}Ti of $I = 7/2$; individual hyperfine lines are labeled by the quantum number F. The $\Omega = 1$ and 3 spectra show a classic Landé pattern, while $\Omega = 2$ is less well-defined, in part because of overlapping transitions. These spectra are each the result of a single scan with a width of 110 MHz and a duration of 70 s.

fixed to those established by the optical study of Amiot et al. (1995). For the two species without nuclear spin, satisfactory fits (25 and 31 kHz for ^{46}TiO and ^{50}TiO, respectively) were achieved with only B, D, A_D, and λ_D as variables. For ^{47}TiO and ^{49}TiO, the magnetic hyperfine parameters a, b, and $(b + c)$, as well as the electric quadrupole coupling constant, eQq, were additionally fitted. Furthermore, as found for VN in its $X\ ^3\Delta_r$ state (Flory & Ziurys 2007), a perturbation term Δa had to be included for the $\Omega = 2$ component. As has been noted by these authors and others (e.g., Azuma et al. 1989), the hyperfine structure of the $\Omega = 2$ level is perturbed by a nearby $^1\Delta$ excited state, in this case, the $a^1\Delta$ term. Isoconfigurational mixing occurs, generating a cross term between the spin–orbit and Fermi contact Hamiltonians. Without this additional parameter, a reasonable fit to the $\Omega = 2$ hyperfine data could not be accomplished. With these additional constants, the rms values of the fits for ^{47}TiO and ^{49}TiO analyses were 71 and 73 kHz, respectively.

Table 2 summarizes the results of the spectroscopic analyses for the four isotopologues. We also list in the table the hyperfine constants a, b, and eQq obtained by Fletcher et al.

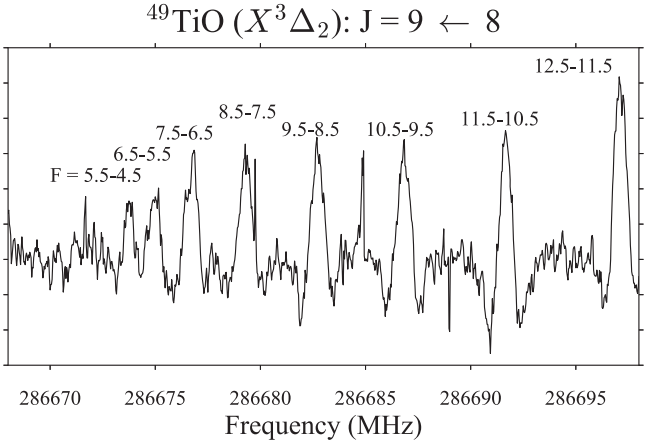

Figure 3. Millimeter/submillimeter direct absorption spectrum of the $J = 9 \leftarrow 8$ rotational transition of ^{49}TiO ($X^3\Delta_r$) near 286 GHz in the $\Omega = 2$ ladder only. At the lower frequency, the hyperfine octet is distinct, but the spacing between lines decreases with decreasing F quantum number (see Figure 2). This spectrum was generated in a single scan of 70 s with a width of 30 MHz.

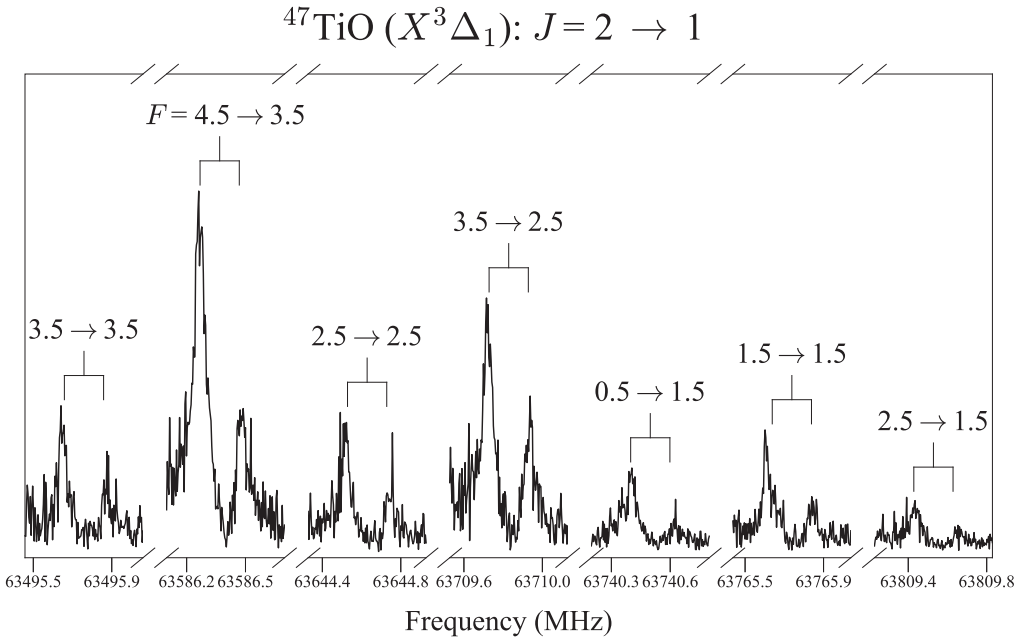

Figure 4. Fourier transform millimeter-wave (FTmmW) spectrum of the $J = 2 \rightarrow 1$ rotational transition of ^{47}TiO ($X^3\Delta_1$) in the $\Omega = 1$ ladder near 62 GHz. All seven measured hyperfine components are shown, labeled by the quantum number F. There are six frequency breaks in the spectrum to display all the lines. Doppler doublets are indicated by brackets. Each line was created from a scan with a width of 600 kHz using between 3000 and 20,000 scan averages.

Table 2
Spectroscopic Constants for TiO Isotopologues ($X^3\Delta_r$)

Parameter	Present Work				Previous Work[a]
	^{46}TiO	^{47}TiO	^{49}TiO	^{50}TiO	^{47}TiO
B	16177.0691(19)	16088.3416(20)	15921.9273(17)	15843.7944(22)	⋯
D	0.0185190(50)	0.0183079(57)	0.0179366(48)	0.0177631(53)	⋯
A	1518477.2[b]	1518477.2[b]	1518477.2[b]	1518477.2[b]	⋯
A_D	−0.81850(42)	−0.80639(51)	−0.78417(42)	−0.77366(49)	⋯
λ	52380.0[b]	52380.0[b]	52380.0[b]	52380.0[b]	⋯
λ_D	0.01885(75)	0.0217(23)	0.01897(97)	0.01830(88)	⋯
λ_H	⋯	$-1.11(70) \times 10^{-5}$	⋯	⋯	⋯
a	⋯	−53.36(28)	−53.155(85)	⋯	−54.7(6.3)
Δa	⋯	−18.28(67)	−19.01(36)	⋯	⋯
b	⋯	−235.3(2.1)	−232.94(45)	⋯	⋯
$b + c$	⋯	−232.19(46)	−231.94(17)	⋯	−232(18)
$(b + c)_D$	⋯	−0.0178(15)	⋯	⋯	⋯
eQq	⋯	−54.587(86)	−44.72(10)	⋯	−49(93)
rms	0.025	0.071	0.073	0.031	6.7

Notes. In MHz; the errors quoted are 3σ.
[a] Fletcher et al. (1993).
[b] Held fixed to value from Amiot et al. (1995).

(1993) for ^{47}TiO. The two sets of values agree well within the uncertainties.

5. DISCUSSION

This study has generated the first set of accurate rotational frequencies and spectroscopic constants for the rare isotopologues of titanium oxide. The possibility of measuring titanium isotope ratios now exists at millimeter wavelengths, which potentially could test theories of nucleosynthesis in stellar envelopes. Although rotational lines generated by these species are likely to be very weak, new-generation telescopes such as ALMA may be sufficiently sensitive to detect these rare species. The envelope of VY CMa would be an excellent target source.

The complicated ^{47}TiO and ^{49}TiO hyperfine patterns can be understood in terms of the competing constants a, b, and c. In the case of both species (see Table 2), $2a \approx -106$ MHz, which is lower than $(b + c) \approx -231$ MHz. The basic form of the diagonal matrix element for the magnetic hyperfine interaction is

$$\{[a\Lambda + (b + c)\Sigma]\Omega[F(F + 1) - J(J + 1) - I(I + 1])\}/2J(J + 1). \quad (2)$$

For $\Omega = 2$, $\Sigma = 0$, and the hyperfine pattern is entirely determined by a, which, because it is smaller than $(b + c)$, generates a more compact pattern. For $\Omega = 1$ and 3, the $(b + c)$ term dominates. For $\Omega = 1$, $\Sigma = -1$, and $(b + c)$ Σ reverses sign with respect to $a\Lambda$, reversing the hyperfine

pattern relative to $\Omega = 2$ and 3. In the case of $\Omega = 3$, $a\Lambda$ and $(b + c)\Sigma$ have the same (negative) sign, leading in this case to a significantly larger splitting. The higher value of Ω also contributes to the extent of the splitting; see Equation (2).

The electron configuration of TiO is $\delta^1\sigma^1$ (e.g., Merer 1989). From the Fermi contact parameter, $b_F = b + c/3 \approx b$, the amount of atomic titanium 4*s* orbital character can be estimated by comparison with the atomic value, namely

$$[b_F(\mathrm{TiO})]/[(1/2S)b_F(\mathrm{Ti})]. \quad (3)$$

Here S is the total spin. (The factor $1/2S$ arises because of differences in the microscopic versus macroscopic form of the Hamiltonian for the Fermi contact interaction, $\langle S\|\boldsymbol{s}_i\|S\rangle = (1/2S)\langle S\|\boldsymbol{S}\|S\rangle$; see Flory & Ziurys 2007). For titanium, the atomic $b_F = -782$ MHz (Morton & Preston 1978). Therefore, the *s* orbital is approximately 60% 4*s* character. The remaining contribution to the *s* orbital is likely from the 3*d* atomic orbital, suggesting a fair amount of *sd* hybridization in the molecule. Note that both ^{47}TiO and ^{49}TiO give virtually equivalent results, as expected.

The validity of the perturbation hyperfine constant Δa can be evaluated by using it to estimate the energy of the nearby $a^1\Delta$ state, which has been experimentally measured to be 3444 cm^{-1} (Kaledin et al. 1995). As described by Flory & Ziurys (2007) and by Balfour et al. (1993), an expression Δa can be obtained from second-order perturbation theory:

$$\Delta a = \frac{4A(b - c)}{\Delta E(^1\Delta - {}^3\Delta)}. \quad (4)$$

Here A is the spin–orbit constant of the $X^3\Delta_r$ state (see Table 2) and $\Delta E(^1\Delta–^3\Delta)$ is the energy difference between the $a^1\Delta_2$ and $X^3\Delta_2$ levels. Using the values in Table 2, the energy of the excited $a^1\Delta$ state is calculated to be ~2570 cm^{-1} above the $\Omega = 2$ level, or ~2670 cm^{-1} above the $\Omega = 1$ level. This estimate is within 22% of the actual value, giving credence to the Δa term.

This research is supported by NSF grants AST-1515568 and CHE-1565765.

REFERENCES

Amiot, C., Azaroual, E. M., Luc, P., & Vetter, R. 1995, JChPh, 102, 4375
Amiot, C., Luc, P., & Vetter, R. 2002, JMoSp, 214, 196
Azuma, Y., Barry, J. A., Lyne, M. P. J., et al. 1989, JChPh, 91, 1
Balfour, W. J., Merer, A. J., Niki, H., Simard, B., & Hackett, P. A. 1993, JChPh, 99, 3288
Barnes, M., Merer, A. J., & Metha, G. F. 1996, JMoSp, 180, 437
Brown, J. M., & Carrington, A. 2003, Rotational Spectroscopy of Diatomic Molecules (Cambridge: Cambridge Univ. Press)
Clayton, D. 2003, Handbook of Isotopes in the Cosmos: Hydrogen to Gallium (Cambridge: Cambridge Univ. Press)
DeBeck, E., Vlemmings, W., Muller, S., et al. 2015, A&A, 580, A36
Fletcher, D. A., Surlock, C. T., Jung, K. Y., & Steimle, T. C. 1993, JChPh, 99, 4288
Flory, M. A., & Ziurys, L. M. 2007, JMoSp, 247, 76
Greber, N. D., Dauphas, N., Millet, M. A., & Puchtel, I. S. 2016, in 47th Lunar and Planetary Science Conference, 1903, 1448
Kaledin, L. A., McCord, J. E., & Heaven, M. C. 1995, JMoSp, 173, 499
Kaminski, T, Gottlieb, C. A., Menten, K. M., et al. 2013, A&A, 551, A113
Kobayashi, K., Hall, G. F., Muckerman, T., Sears, T. J., & Merer, A. J. 2002, JMoSp, 212, 133
Merer, A. J. 1989, ARPC, 40, 407
Miceli, M., Sciortino, S., Troja, E., & Orlando, S. 2015, ApJ, 805, 120
Min, J., Halfen, D. T., & Ziurys, L. M. 2014, CPL, 609, 70
Morgan, W. W., & Keenan, P. C. 1973, ARA&A, 11, 29
Morton, J. R., & Preston, K. F. 1978, JMagR, 30, 577
Namiki, K., Saito, S., Robinson, J. S., & Steimle, T. C. 1998, JMoSp, 191, 176
Nittler, L. R., & Hoppe, P. 2005, ApJL, 631, L89
Prantzos, N., Arnould, M., & Arcoragi, J.-P. 1987, ApJ, 315, 209
Ram, R. S., Bernath, P. F., & Wallace, L. 1996, ApJS, 107, 443
Sun, M., Apponi, A. J., & Ziurys, L. M. 2009, JChPh, 130, 034309
Wade, R. A., & Horne, K. 1988, ApJ, 324, 411
Wyckoff, S., & Wehinger, P. 1972, ApJ, 178, 481
Ziurys, L. M., Barclay, W. L., Jr., Anderson, M. A., Fletcher, D. A., & Lamb, J. W. 1994, RScI, 65, 1517